Experiments on Image Compression using Morphological Pyramids

Fang-Kuo Sun

The Analytic Sciences Corp.
55 Walkers Brook Drive
Reading, MA. 01867

Petros Maragos

Division of Applied sciences
Harvard University
Cambridge, MA 02138

ABSTRACT

In this paper, the concept of morphological pyramids for image compression and progressive transmission is discussed. Experimental results from applying these pyramids to three real images, a satellite cloud image, a tank image from arerial photography and a NMR skull image, are presented. For lossless compression, no reduction in total (first order) entropies of error pyramids derived from the original images are observed in all three cases. However, high quality reconstructions of original images from the corresponding error pyramids can be achieved with significant reduction in total entropies.

1. INTRODUCTION

In the last ten years, autoregressive modeling and orthogonal transformations such as Fourier or Karhunen-Loeve transformations have provided basic theoretical foundations for most of the research in image compression and coding. Most of these approaches exploit primarily the algebraic structure of signals. However, since image objects are most naturally perceived as geometrical pattern, there is a need for representations that emphasize geometric rather than algebraic structures. Mathematical morphology provides a geometric representation of an image by summarizing its shape and conveying its size, orientation and connectivity (Ref. 1). Mathematical morphology is a set-theoretic method for image analysis, which was created around 1964 at the Paris School of Mines, France, by G.Matheron and J. Serra. The objective is to provide a quantitative description of geometric structures of an image. The general approach is to probe and transform an image object with different patterns of predefined shapes, called structuring elements.

Pyramid representations are important tools in computer vision for image filtering and analysis at multiple scales, and are applied extensively in image compression and progressive transmission (Ref. 2, 3). The most common approach is to linearly convolving the image with Gaussian functions of increasing standard deviations. Recently, theoretical research on morphological pyramids and hierarchical image representations have been reported (Refs. 4,5, 6). In this paper, we explore some basic properties of various morphological pyramids for image compression and progressive transmission via experiments on several real images. Morphological opening, which can be treated as a shape filter, is the basic operator for smoothing. The advantages of morphological operators are their direct geometric interpretations, and simplicity and efficiency in implementation.

This paper is organized as follows. In Section 2, fundamental operators in mathematical morphology are briefly discussed, and the idea and definitions of various morphological pyramids are introduced. Section 3 presents some experimental results from applying morphological pyramids to three real images. The result is compared to a linear pyramid. Properties of morphological error pyramids are examined through numerical results.

Decimation is accomplished by subsampling, e.g. retaining every other pixels for a binary structuring element of 3x3 square.. We will refer this pyramid as the smoothed pyramid in the remaining discussion.

Intutively, the decimated smoothed image represents the best estimate of the original image at the given (size) resolution and can be used for reconstructing the original image. In image compression for storage or transmission, it is more efficient to introduce a corresponding error pyramid defined as the difference between two images before and after the smoothed operation, e.g. Gaussian error pyramid in the linear case (Ref. 3). A morphological (direct) error pyramid is defined by $\mathfrak{E} = \{D_{(i-1)\cdot g}, i = 1, 2, ...\}$, where

$$D_{(i-1)\cdot g} = f_{(i-1)\cdot g} - (f_{(i-1)\cdot g})_g \qquad (2\text{-}5)$$

Each element of the the error pyramid is the (size) residual respresenting the detail of the original image. Normally, these residual images are very sparse, and contain much less entropy than the original images. It should be noted that unlike the residual derived from a linear smoother, since opening can not increase the value at each pixel location, the dynamic range of $D_{(i-1)\cdot g}$ can not be greater than that of the original image. Theoretically, if the smoothed (open) operation is a perfect frequency (size) band-pass filter, then there is no loss of information in the decimation process, and the error pyramid will be sufficient for reconstructing the original image. In practice, the reconstruction from this error pyramid will be imperfect due to the non-ideal smoothed operation. However, as discussed in the next section, the reconstructions are near perfect for all cases considered with added benefit of greater reduction in entropy.

For perfect reconstruction, a modified (lossless) error pyramid can be defined as follows:

(1) Initialization:
$$f_{0\cdot g} = F$$

(2) open image $f_{(i-1)\cdot g}$ by g and denoted by $(f_{(i-1)\cdot g})_g$

(3) $f_{i\cdot g}$ = decimated($(f_{(i-1)\cdot g})_g$)

(4) $F'_{i\cdot g}$ = upsampled($f_{i\cdot g}$)

(5) $R_{i\cdot g} = f_{(i-1)\cdot g} - F'_{i\cdot g}$

(6) Repeat (2) to (6) until $f_{i\cdot g}$ vanishes

Obviously, the upsampled image $F'_{i\cdot g}$ is intended to be an estimate of the smoothed input image $(f_{(i-1)\cdot g})_g$. The price for obtaining the perfect reconstruction is that $F'_{i\cdot g}$, in general, yields more entropy than $(f_{(i-1)\cdot g})_g$ as shown empirically in the next section.. Fig 2-1 shows the algorithmatic flow for the lossless error pyramid construction. The function, upsampled, is to provide the best estimate of the smoothed image by interpolation. The effect of using different interpolation schemes, for example, linear vs nonlinear (morphological), is discussed in the next section..

This lossless error pyramid, $\{R_{i\cdot g}, i = 1, 2, ..., K\}$, is used for encoding. The following proposition will show that $\{R_{i\cdot g}, i = 1, 2, ..., K\}$ is sufficient for recontructing the original image.

Proposition 2.1: $\{R_{i\cdot g}, i = 1, 2, ..., K\}$ is sufficient for reconstructing the original image F.

3. EXPERIMENT RESULTS

Three 256x256 images as shown in Fig. 3-1 are used for analysis. The cloud image is a 8 bit visible band satellite imagery. The 8 bit tank image is obtained from aerial phtography. The human skull is a 12 bit NMR image. Except for the NMR image, both cloud and tank images contains many small details. These are reflected by their raw (first order) entropy content as shown in the Table 3.1. Fig. 3-2 shows the histogram of the cloud image. Notice that intensity values are rather uniformly distributed between 55 and 195, and the largest percentage is about 1.1%. Due to the space limitation, only the pictural results from the cloud image will be shown here.

A morphological image processing software package implemented on Alliant Fx8 at TASC is applied to these images. In this software package, the high level routines are written in C, but the lower level computation routines are written in Fortran to fully utillize the existing multiple CE's on Fx8 for speeding up the processing.

An example of the smoothed morphological pyramid is shown as the diagonal blocks in Fig. 3-3. The structuring element used for morphological smoothing is a 3x3 binary square. Opening removes any features smaller than 3x3 square as evidenced in the upper triangular blocks of Fig. 3-3. These small features are then captured by the (direct) residual, i.e. the difference between the original and opened images as shown in Fig. 3-4 (a) for the first 256x256 block. For comparison, the linear residual (where the smoothing is carried out by a 3x3 mean (mathematical average) local operator is shown in Fig. 3-4 (b). Structurewise, they are very similar. However, the dynamic ranges for morphological and linear residuals are [0, 138] and [-72, 111], respectively. The negative pixel values are direct results of mathematical average. The entropies for the corresponding residuals of different images are summarized in Table 3-2. In all cases, it shows that entropies of morphological residuals are smaller than those of linear cases. The significant smaller entropy for the residual image of the skull image is due to the fact that geometically the original skull image mainly consists of large smooth objects.

As noted in the previous section, the reconstruction of the original image from its direct error pyramid is imperfect. Fig. 3-5 shows the reconstructed cloud image using the 256x256 and 128x128 direct residuals.and the 64x64 diagonal block in Fig. 3-3. The visual quality of this reconstruction is very good. Note that this is also the case for both tank and skull images. Quantitatively, the signal to noise ratio measured as

$$\text{S/N (in db)} = 20 * \text{Log}_{10}\left(\frac{\text{peak to peak signal level}}{\text{standard deviation of the error}}\right);$$

$$\text{standard deviation of the error} = \sqrt{\frac{\sum (x_{i,j}^{ori} - x_{i,j}^{rec})^2}{\text{\# of pixels}}} \qquad (3\text{-}1)$$

where x_{ij}^{ori} and $x_{i,j}^{rec}$ are pixel values at location (i, j) for the original and reconstructed images, respectively, are 28 db , 24 db and 30 db for the cloud, tank and skull images. The total entropies (cloud image: 5.83 bits/pixel, tank image: 5.65 bit/pixel, skull image: 3.98 bit/pixel) for images used in the reconstruction are smaller than those for the original images. In general, the tank image exhibits the most significant degradation, and the skull image has a 42% reduction in entropy.

In Fig. 3-3, each of the lower triangular blocks is the upsampled version of the smoothed version to its right. To fill up the "holes" (pixels with zero values) in these block,

5. Eichmann, G, Lu, C., Zhu, J. and Li, Y., " Pyramidal Image Processing Using Morphology", SPIE vol. 974 Applications of Digital Image Processing XI, 1988.

6. Maragos, P. "Morphology-based Symbolic Image Modeling, Multi-scale Nonlinear Smoothing, and Pattern Spectrum, " IEEE Computer Society Conference on Computer Vision and pattern Recognition, Ann Arbor, Mi., June, 1988.

7. Sun, F.K. and Rubin, S. L., " Algorithm Development for Autonomous Image Analysis, Based on Mathematical Morphology," SPIE vol. 845 Visual Communications and Image Processing II, 1987.

8. Haralick, R.M., Lin, C., Zhuang, X.," Multiresolution Morphology, " Proceeding first International Conference on Computer Vision, IEEE Computer Soc. Press, New York, 1987

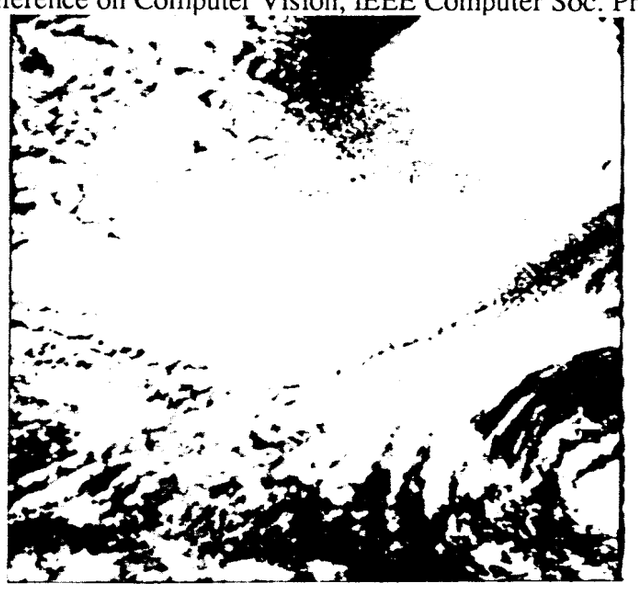

Fig. 3-1: Satellite cloud image,
tank image,
and NMR skull image

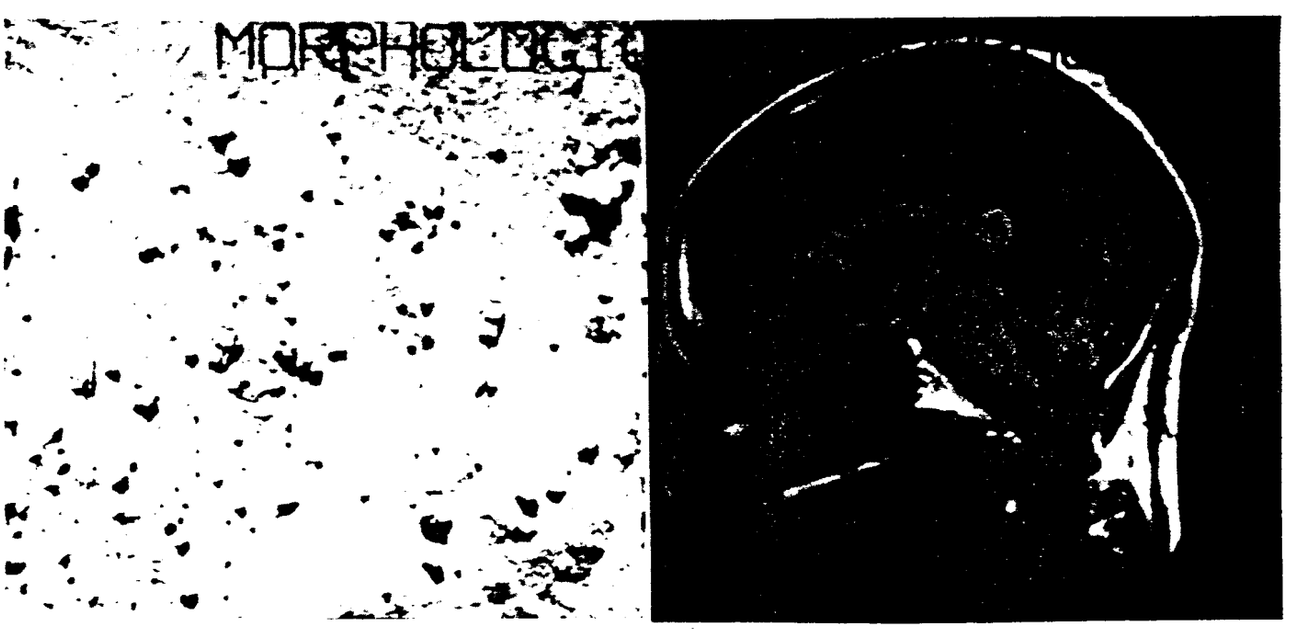

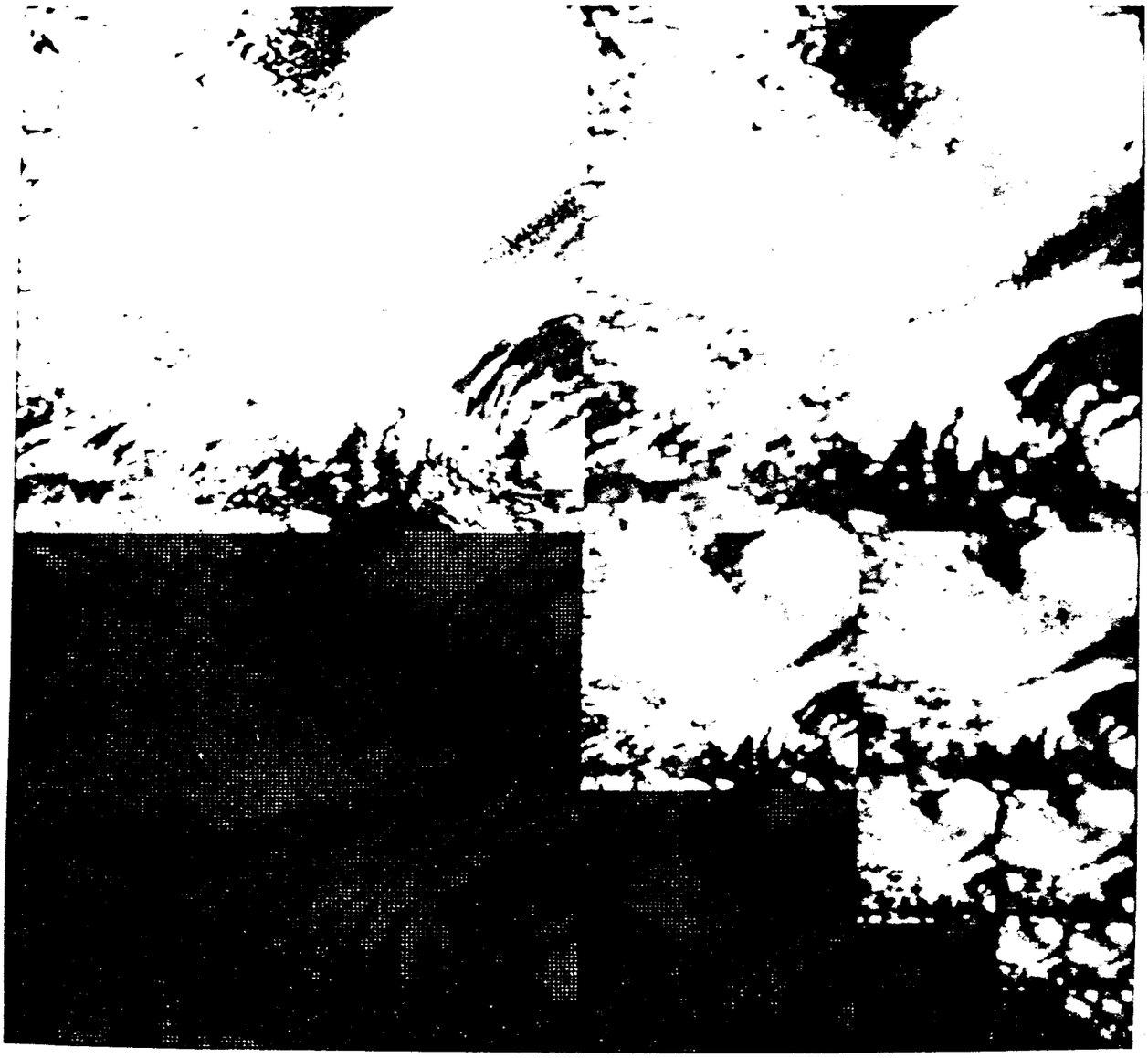

Fig. 3-3: Smooth morphological pyramid for the cloud image